Intermetallics 92 (2018) 84–92

Contents lists available at ScienceDirect

Intermetallics

journal homepage: www.elsevier.com/locate/intermet

On the influence of Mn on the phase stability of the $CrMn_xFeCoNi$ high entropy alloys

K.A. Christofidou[a], E.J. Pickering[b], P. Orsatti[a], P.M. Mignanelli[a], T.J.A. Slater[b], H.J. Stone[a], N.G. Jones[a,*]

[a] Department of Materials Science and Metallurgy, University of Cambridge, 27 Charles Babbage Road, Cambridge, CB3 0FS, UK
[b] School of Materials, University of Manchester, Oxford Road, Manchester, M13 9PL, UK

ARTICLE INFO

Keywords:
High-entropy alloy
Phase stability
Heat treatment
Electron microscopy

ABSTRACT

The *fcc* phase of the equiatomic high entropy alloy, CrMnFeCoNi, has been recently shown to be unstable at temperatures below 800 °C. However, the stability of the constituent CrFeCoNi quaternary alloy, which forms the basis of many other high entropy systems, remains under debate and the existing literature contains very little long duration heat treatment data. Here, the phase equilibria of CrFeCoNi and $CrMn_{0.5}FeCoNi$ are assessed following 1000 h exposures at 500, 700 and 900 °C. Prior to thermal exposure the cast alloys were homogenised and shown to exist as single phase *fcc* solid solutions. In line with previous reports, Cr rich particles were observed on the grain boundaries following the prolonged exposures but detailed electron microscopy showed that these features were $M_{23}C_6$ carbides resulting from the unintentional incorporation of C during production. However, no evidence was found for any other phase formation during the heat treatments of either alloy, in direct contrast to the results for CrMnFeCoNi. Consequently, it is concluded that, within the limits of the temperature and times considered, the solid solution phases of both CrFeCoNi and $CrMn_{0.5}FeCoNi$ are stable and that Mn has a destabilising influence when present in sufficient concentrations. This change in behaviour occurs for a Mn content between 11.1 and 20 at.%.

1. Introduction

Within the last two years, experimental results have shown that the equiatomic high entropy alloy, CrMnFeCoNi, originally thought to be a stable single phase solid solution, is susceptible to the formation of the topologically close packed sigma phase at temperatures between 500 and 800 °C [1–3]. It has also been identified that this alloy undergoes more complex phase decompositions at lower temperatures resulting in multiple phases [2,4].

In contrast, the CrFeCoNi quaternary alloy, which is the basis of many other high entropy alloy systems, is still widely regarded to be stable as a single solid solution phase at all temperatures below the solidus. Several studies have reported that CrFeCoNi exists as a single *fcc* solid solution phase based on data from cast material, gathered using laboratory diffraction techniques and relatively low-resolution electron microscopy [5–8]. Other investigations have utilised various annealing heat treatments prior to characterisation, yet the single solid solution phase remains the only observed microstructural constituent [5,9,10]. One study also used neutron diffraction and anomalous X-ray scattering to study the structure of the material following heat treatment at 480 °C for 336 h. Again, the data indicated that only a single *fcc* structure was present and that no ordered phases, such as Ni_3Fe, had formed [10].

However, more recently, the apparent stability of this alloy has also been questioned by the results of publications that have studied the material with higher resolution techniques. For example, a suction-cast sample of CrFeCoNi, thought to be homogeneous from scanning electron microscopy data, was found to contain compositional fluctuations above the measurement error, when characterised using atom probe tomography [11]. Similarly, analysis of the peak profiles obtained from high-energy synchrotron diffraction revealed that the as-cast material contained at least two different *fcc* phases, with very similar lattice parameters [12].

It should be noted that materials studied in an as-cast state are highly likely to contain solidification-induced microsegregation and, therefore, the presence of these inhomogeneities will be reflected in the data gathered from any given technique that is capable of characterising the material at a corresponding length scale. The existence of elemental segregation may also influence the behaviour of the material during subsequent investigations, for example during low or

* Corresponding author.
E-mail address: ngj22@cam.ac.uk (N.G. Jones).

http://dx.doi.org/10.1016/j.intermet.2017.09.011
Received 11 August 2017; Received in revised form 24 August 2017; Accepted 14 September 2017

intermediate temperature heat treatments. Avoidance of this issue is of critical importance to phase equilibria research, as highlighted by two recent reviews [13,14], both of which emphasise the need for studies of multi-component alloys to start with material that is as homogeneous as possible. Nevertheless, recent transmission electron microscopy results from CrFeCoNi have led to the suggestion that phase decomposition may be occurring in these materials during prolonged high temperature heat treatments [15].

Rather surprisingly, there is relatively little data in the literature that relates to the influence of long-term heat treatments at intermediate temperatures on the constituent phases of CrFeCoNi. One study that has characterised as-cast material subsequently exposed for 800 h at 750 °C in air reported data consistent with a single solid solution phase from scanning electron microscopy and X-ray diffraction data [16]. However, characterisation of the material in a transmission electron microscope revealed lenticular features within an *fcc* matrix. High resolution imaging of these features did not identify any clear interfaces and showed only small distortions of the lattice, on the order of 3 p.m. From these results, the authors concluded that CrFeCoNi was metastable at 750 °C and they had observed elemental clustering during the initial stages of phase decomposition, although no chemical data relating to the features were reported. In addition, when 2.4 at.% Al was incorporated into the alloy, a Cr rich phase was observed on the grain boundaries following exposure at 750 °C, which based on its measured composition, was suggested to be the sigma phase [16].

Recently, a dedicated HEA thermodynamic database has been developed (ThermoCalc TCHEA) and has been used to look at the effect of each constituent component on the phase equilibria in the CrMnFeCoNi system [17]. The thermodynamic predictions produced in this study suggested that Co and Ni support the formation of a single *fcc* phase, Fe has little effect, whilst Mn and particularly Cr destabilise the single phase state. Experimental results from eight different alloys, heat treated for times between 48 and 144 h at either 1000 or 1100 °C, were used to validate the fidelity of the predictions. Comparison of the experimental findings to the theoretical predictions revealed that the extent of the *fcc* solid solution was well described but that the database underpredicted the stability of the sigma phase. Thorough assessments of the accuracy of thermodynamic predictions, such as those presented in Ref. [17], are critical if these databases are to form the basis for alloy design activities.

Another interesting feature arising from these thermodynamic calculations were the changes in the phase equilibria for the quaternary CrFeCoNi alloy as a function of temperature [17]. As would be expected, at high temperatures ($T > \approx 650$ °C) a single *fcc* solid solution was predicted but at lower temperatures, multiple phases were predicted, including two *bcc* phases and a second *fcc* phase. Further to this, the incorporation of a small amount of Mn was predicted to introduce the sigma phase as well. However, these particular alloys were not fabricated or characterised in Ref. [17], nor were any experimental data obtained at temperatures below 1000 °C, and so these predictions have not been verified.

It is evident from this short review of the literature that there are many discrepancies in the published data with respect to the stability of the CrFeCoNi alloy. Clearly, this is a key issue to resolve in understanding the stability of the single *fcc* phase, not only from a fundamental standpoint but also given that this quaternary alloy forms the basis of several different high entropy alloy systems. In addition, if the quaternary alloy is established to be stable as a single solid solution phase, then it would demonstrate that the Mn additions are responsible for destabilising that phase and promoting the formation of the sigma phase in the CrMnFeCoNi system, consistent with thermodynamic predictions. Therefore, in the present work, we investigate the influence of Mn on the phase stability of $CrMn_xFeCoNi$ HEAs at temperatures below 1000 °C by studying two alloys, with $x = 0$ & 0.5, and comparing the results with those obtained from the equiatomic alloy, $x = 1$, which were previously reported in Ref. [1].

2. Experimental method

To investigate the role of Mn on the phase stability of alloys in $CrMn_xFeCoNi$ HEAs, two 50 g ingots were arc melted from pure elements under an inert atmosphere. The nominal Mn content of these alloys was 0 and 11.1 at.%, corresponding to CrFeCoNi and $CrMn_{0.5}FeCoNi$ respectively. To enhance the macroscopic homogeneity of the ingots, each alloy was inverted and remelted a total of five times. In line with previous work [2], the cast alloys were homogenised for 100 h at 1200 °C inside evacuated and argon backfilled quartz ampoules. Several transverse sections, approximately 10 mm thick, were taken from the homogenised ingots, each of which was encapsulated as above and thermally exposed at either 500, 700 or 900 °C for 1000 h.

Material at each stage of the process was characterised using backscattered electron imaging in an FEI Nova NanoSEM 450 scanning electron microscope (SEM), which was also fitted with a Bruker xFlash 100 detector, enabling energy dispersive X-ray (EDX) mapping of the elemental distributions. Calorimeteric data was acquired between room temperature and 1450 °C using a Netzsch 404 differential scanning calorimeter at heating and cooling rates of 10 °C min^{-1} under flowing argon. X-ray diffraction patterns were gathered using a Bruker D8 diffractometer, with a Ni filtered Cu source, between angles of 20 and 120° 2θ. Phase identification and lattice parameters were obtained from the diffraction data using the Pawley model in the TOPAS-Academic software.

Higher resolution studies of the alloys were performed using transmission electron microscopy. 3 mm discs were removed from material in different heat treatment conditions and thinned by twin jet electro polishing, using a solution of 10% $HClO_4$ in CH_3OH at −35 °C and an applied potential of 20 V. In addition, several specific sites of interest were extracted from the bulk material through focussed ion beam milling. The electron transparent samples were investigated in an FEI Talos F200X Scanning Transmission Electron Microscope (STEM), equipped with Super EDX detectors, and an aberration corrected FEI Titan, both of which were operated at 200 keV.

3. Results

3.1. As-cast and homogenised material

Backscattered electron (BSE) images of CrFeCoNi and $CrMn_{0.5}FeCoNi$ in the as-cast state are presented in Fig. 1. Both images showed that the materials had a large grained microstructure, with contrast appearing to be driven by crystal orientation rather than compositional variation. Small, black contrast particles were also observed in the as-cast microstructure of both alloys, which were identified to be oxide impurities in line with previous studies [1,18–21]. The bulk compositions of the materials, obtained by averaging five large area (500 × 500 μm) EDX scans, are given in Table 1 and were within ± 1 at.% of the target concentrations for each element in both alloys.

X-ray diffraction patterns for the alloys are shown in Fig. 2 and in the as-cast state the data contained reflections that corresponded to one *fcc* phase, with no other peaks visible above the background. The effect of Mn on the lattice parameter of the *fcc* phase was assessed by full pattern fitting using the Pawley method in TOPAS-Academic. The model for the CrFeCoNi data produced a refined lattice parameter of 3.58 ± 0.01 Å, whilst a value of 3.59 ± 0.01 Å was obtained for $CrMn_{0.5}FeCoNi$. Whilst the BSE images and diffraction data appeared to indicate that both CrFeCoNi and $CrMn_{0.5}FeCoNi$ existed as single phase materials with a homogeneous microstructure in the as-cast state, SEM based EDX mapping showed clear elemental segregation within the grains, consistent with dendritic solidification, Fig. 1.

To remove the solidification induced micro-segregation, the alloys were homogenised at 1200 °C for 100 h. This temperature was chosen to be as close to the solidus temperature of each alloy as possible, found

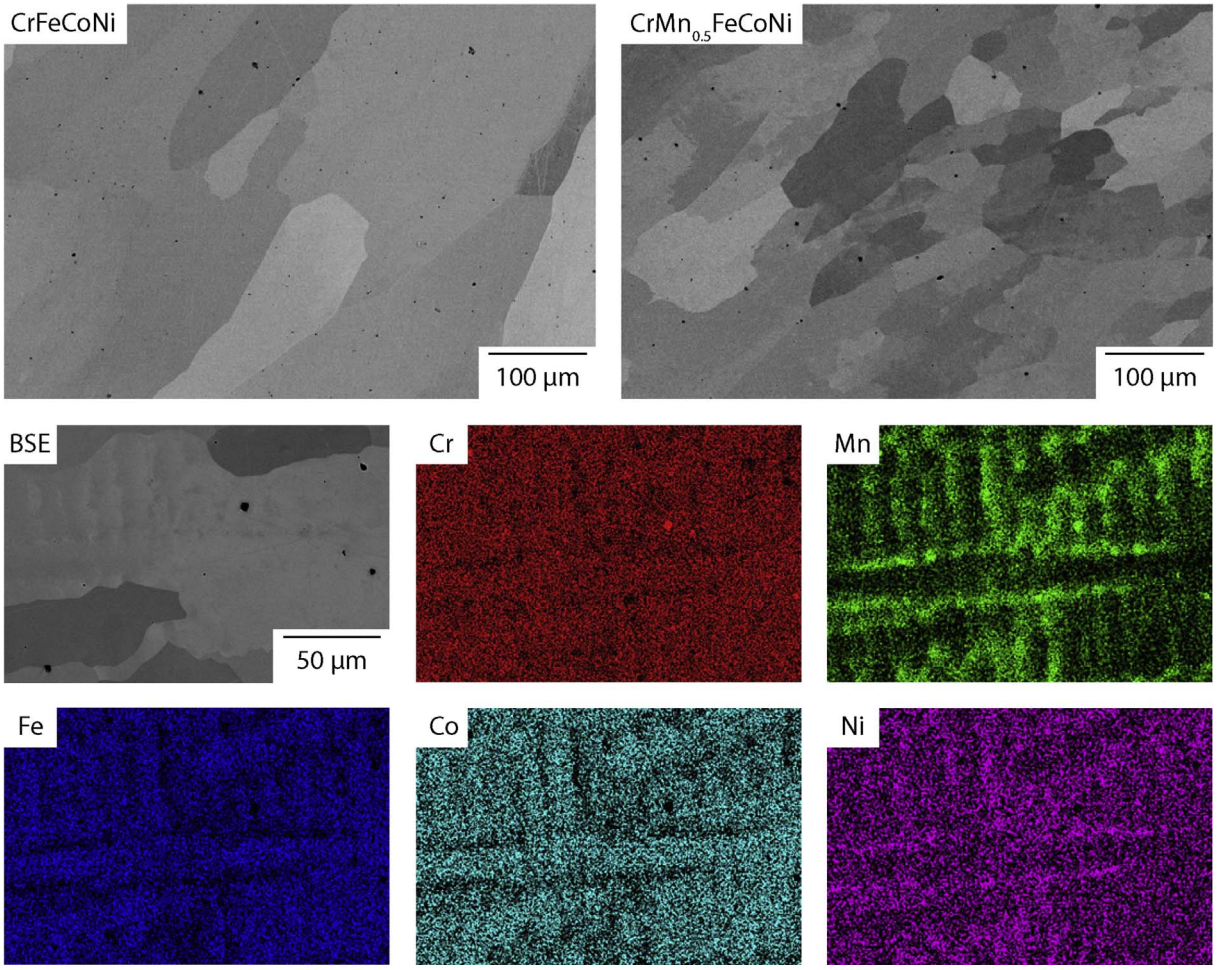

Fig. 1. BSE images of CrFeCoNi and $CrMn_{0.5}FeCoNi$ in the as-cast condition, EDX elemental distribution maps for $CrMn_{0.5}FeCoNi$ as an example of the solidification induced micro-segregation.

Table 1
Bulk compositions of the alloys studied in at.%, as determined from five large area EDX scans (the standard deviation for each element was less than 0.5 at.%).

Alloy	Cr	Mn	Fe	Co	Ni
CrFeCoNi	25	–	26	25	24
$CrMn_{0.5}FeCoNi$	22	11	23	23	21

from calorimetric data to be ~1400 °C for CrFeCoNi and ~1330 °C for $CrMn_{0.5}FeCoNi$, without compromising the operational temperature limit of the fused quartz ampoules and to be consistent with previous work on CrMnFeCoNi [2]. Following the homogenisation heat treatment the grain structures of both alloys were very similar to those observed in the as-cast state. However, unlike the as-cast state, the elemental distribution maps did not show any evidence of the cast dendritic structure. Instead, a homogeneous distribution of each element was observed, as shown in Fig. 3, which corresponds to the same alloy that exhibited the dendritic structure shown in Fig. 1. X-ray diffraction patterns from the two alloys in the homogenised state are shown in Fig. 2 and, again, appear to contain only reflections consistent with a single *fcc* phase.

The constitution of the homogenised material was studied at higher resolution using transmission electron microscopy. Bright field images of material in this condition revealed a reasonably clean microstructure, with a low dislocation density, but that also contained a number of lenticular features, as shown in Fig. 4. To study the lenticular features in more detail, the area within the white box of the bright field image was investigated using HAADF STEM imaging and compositional data acquired using STEM EDX. The features continued to generate contrast in the HAADF imaging mode but, as can be seen from the STEM EDX data in Fig. 4, this was not related to compositional variations. Consequently, it is believed that these features are stacking faults, which have been previously observed in this HEA system [22–24]. Away from the stacking faults, the potential presence of nano-scale clusters was assessed by imaging the atomic columns of the matrix material in HAADF mode. An example of one such image, along with the corresponding Fourier transform, is shown in Fig. 4. Little contrast variation was observed between the different columns, whilst the Fourier transform contained only frequencies that corresponded to an *fcc* structure. Both of these suggested that the material was truly homogeneous with no evidence of any nano-clusters.

3.2. 1000 h heat treated material

To assess the stability of the homogenised solid solution phase in each alloy, small sections were thermally exposed for 1000 h at temperatures of 500, 700 and 900 °C under a protective atmosphere. Following the exposures, additional precipitates were observed on the grain boundaries of both alloys at all of the different temperatures. The precipitates tended to have an elongated morphology, which followed the grain boundary, and had a darker contrast than the surrounding grains when imaged using backscattered electrons. A typical example of these features is given in Fig. 5.

SEM based EDX elemental mapping indicated that these phases

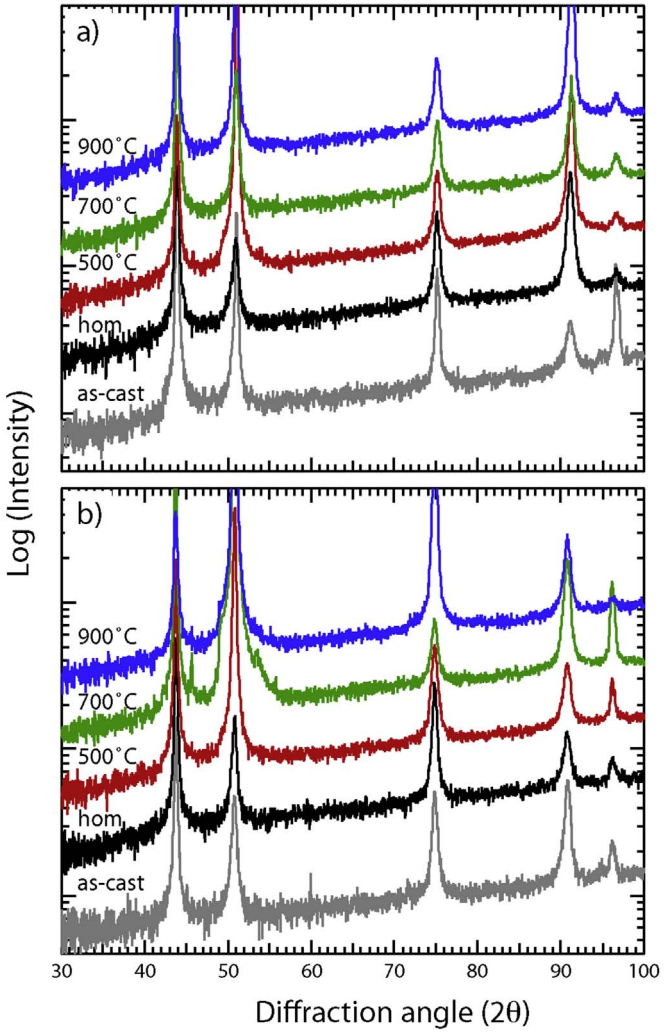

Fig. 2. X-ray diffraction patterns from samples of a) CrFeCoNi and b) $CrMn_{0.5}FeCoNi$ in the as-cast state, following homogenisation (100 h at 1200 °C), and following 1000 h exposure at 500, 700 and 900 °C.

were enriched in Cr whilst being depleted in all of the other intentional alloying elements, Fig. 5. However, if impurity elements, such as C, O, S and N, were also assessed, then the precipitates showed a slight local enrichment of C, suggesting that these precipitates could be a carbide phase. This possibility was also consistent with previous work, as the morphological appearance and elemental distribution of these precipitates were similar to the $M_{23}C_6$ phase reported in CrMnFeCoNi [1]. It should be noted that the elemental distribution maps showed an extremely strong concentration of O, coincident with the Cr enrichment. Such a large local concentration fluctuation, especially at locations a long way from the sample surface did not seem reasonable and, given the proximity of the O Kα emission line to the Cr Lα emission line (less than 50 eV separation), it is more likely that this was simply an erroneous interpretation of the EDX data.

To unambiguously identify the structure of these features, thin foils containing the precipitates were extracted from the heat-treated samples using focussed ion beam milling for study in a transmission electron microscope. A HAADF STEM image of one of the grain boundary precipitates, obtained from the CrFeCoNi alloy exposed at 700 °C, is shown in Fig. 6. The corresponding STEM EDX elemental distribution maps are also shown in Fig. 6 and clearly indicate that the precipitate was enriched in Cr and C. Electron diffraction patterns were obtained from the precipitate from a number of different zone axes, three of which are shown in Fig. 7. These diffraction patterns were consistent with a relatively large *fcc* structure, with a lattice parameter of ~10.6 Å. Similar results were obtained when the grain boundary phases from the $CrMn_{0.5}FeCoNi$ alloy were analysed, Fig. 8, consistent with these features also corresponding to an $M_{23}C_6$ carbide. A quantification of the metallic element content of these carbides, obtained from the STEM EDX analysis is provided in Table 2. The carbon content was not included in this analysis, as its quantification from EDX data, whether STEM or SEM based, is not reliable.

Away from the grain boundary phases, the *fcc* matrices of both alloys were found to be largely unchanged following thermal exposure. SEM, Fig. 5, and TEM, Fig. 6, EDX results showed an even distribution of the constituent elements and the X-ray diffraction patterns shown in Fig. 2 contained no additional peaks that were not consistent with the $M_{23}C_6$ carbides. As such, the results in this study suggest that both CrFeCoNi and $CrMn_{0.5}FeCoNi$ are stable as single phase *fcc* solid solutions within the limits of the temperatures and exposure times considered. However, to support this observation, high resolution images of the materials were obtained, an example of which is shown in Fig. 9. Again, the atom columns were not observed to have any local intensity

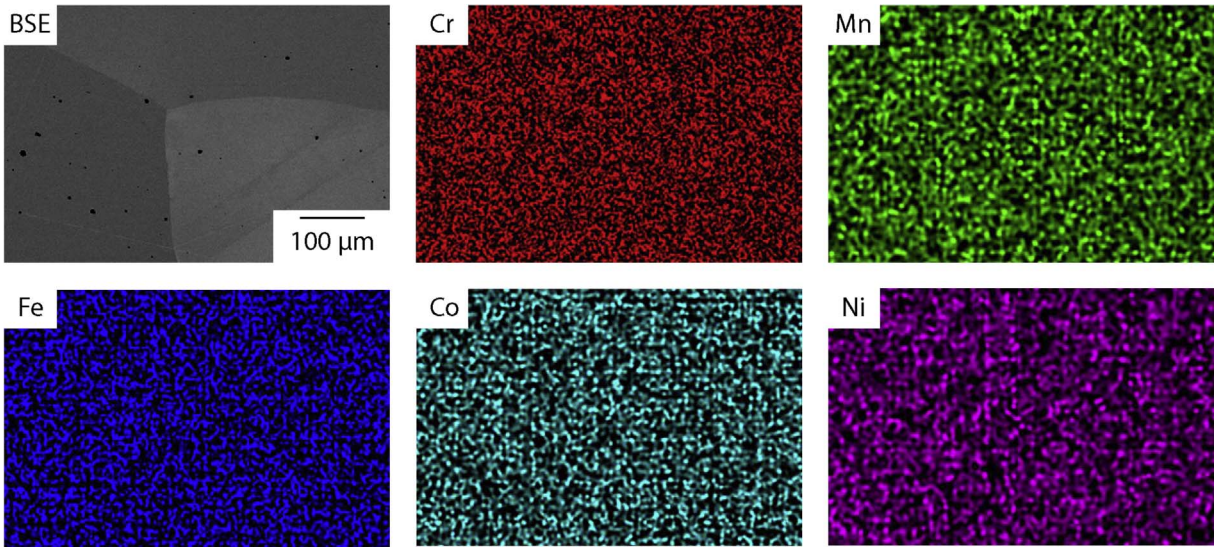

Fig. 3. BSE image and corresponding EDX elemental distribution maps for $CrMn_{0.5}FeCoNi$ in the homogenised condition.

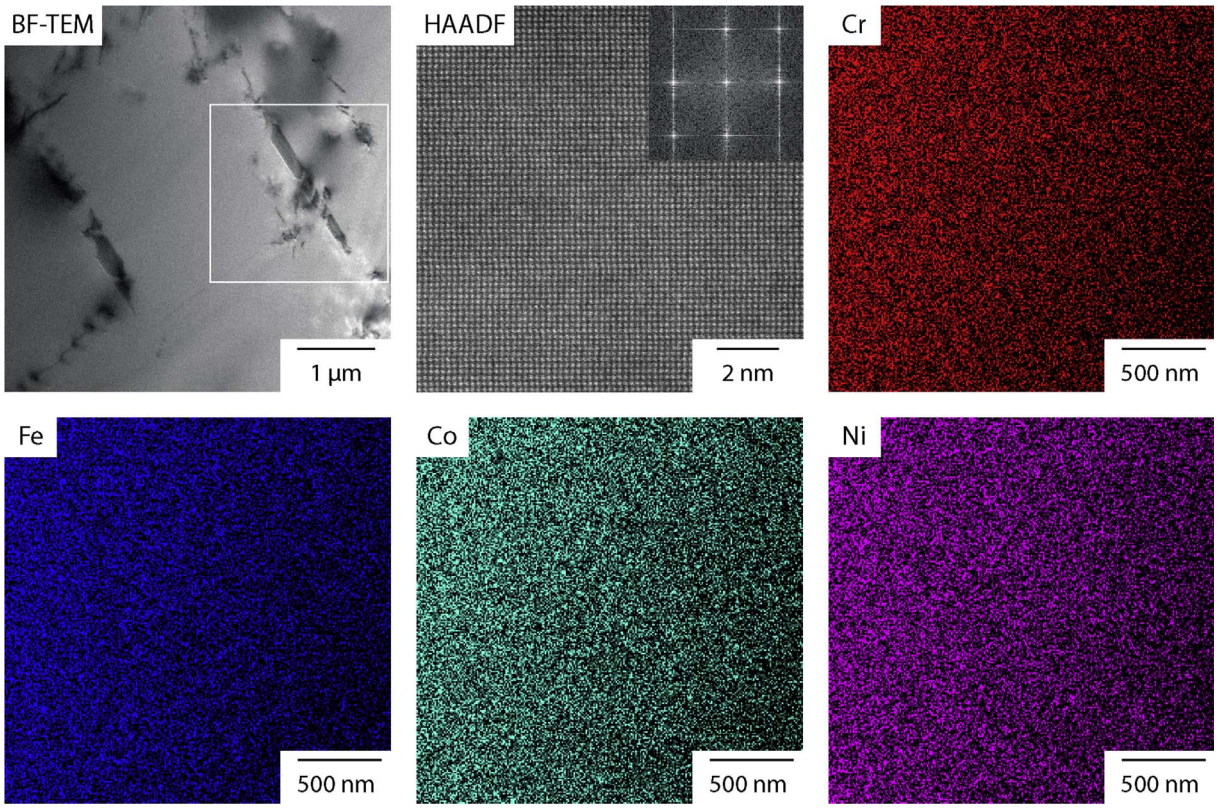

Fig. 4. TEM images of CrFeCoNi in the homogenised condition showing a bright field image containing the lenticular features observed, typical HAADF image of the atom columns from the matrix material with corresponding Fourier transform inset and STEM EDX maps of the area bounded by the white box in the bright field image.

variations and the fast Fourier transform of the data showed only frequencies that corresponded to a single *fcc* structure. Thus, even at an extremely fine length scale these alloys appear to be stable as solid solutions, with no evidence of intermetallic phase formation. Similarly, there is also no evidence of nano-clusters in the heat treated alloys but it must be emphasised that none of the data presented here, nor the techniques used can unambiguously rule out the presence of nano-clusters, either through insufficient spatial resolution or, in the case of atomic-resolution techniques, the relatively small sample volumes analysed.

4. Discussion

The overarching aim of this study was to assess the stability of the single *fcc* solid solution phase in the CrFeCoNi and $CrMn_{0.5}FeCoNi$ HEAs with respect to phase decomposition during long term thermal exposures. Therefore, it was critical to ensure that a single phase state was achieved prior to commencing the tests. In any alloy system, as-cast material is always likely to contain some level of compositional inhomogeneity, which arises as a result of solidification induced micro-segregation. HEAs are not an exception to this situation but what is evident is that care must be taken in assessing their microstructures. For

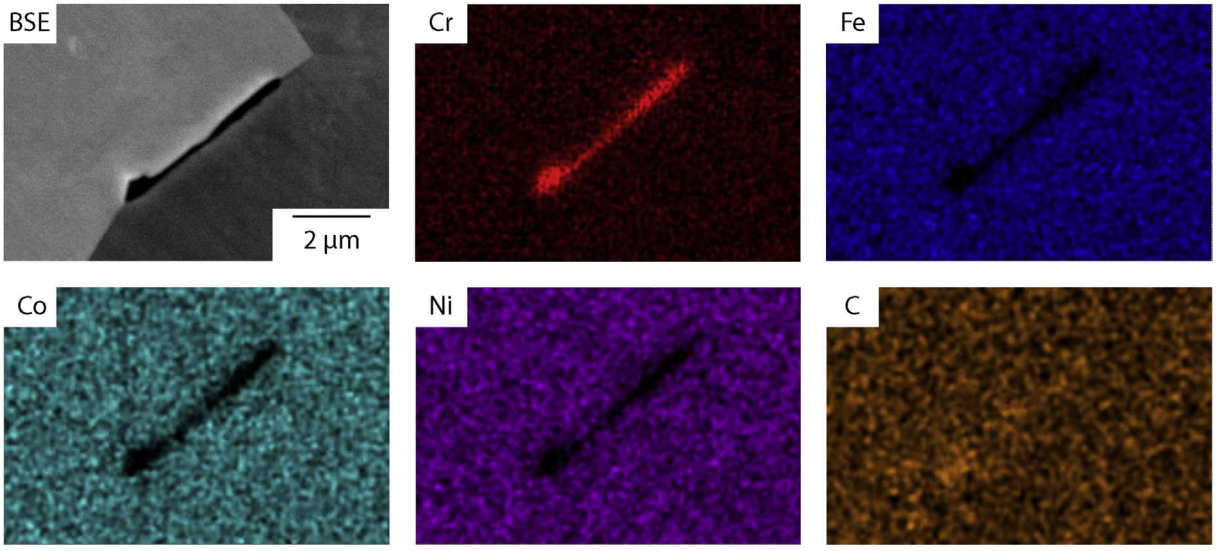

Fig. 5. BSE image and corresponding EDX elemental distribution maps of a grain boundary precipitate observed in CrFeCoNi following a 1000 h exposure at 700 °C.

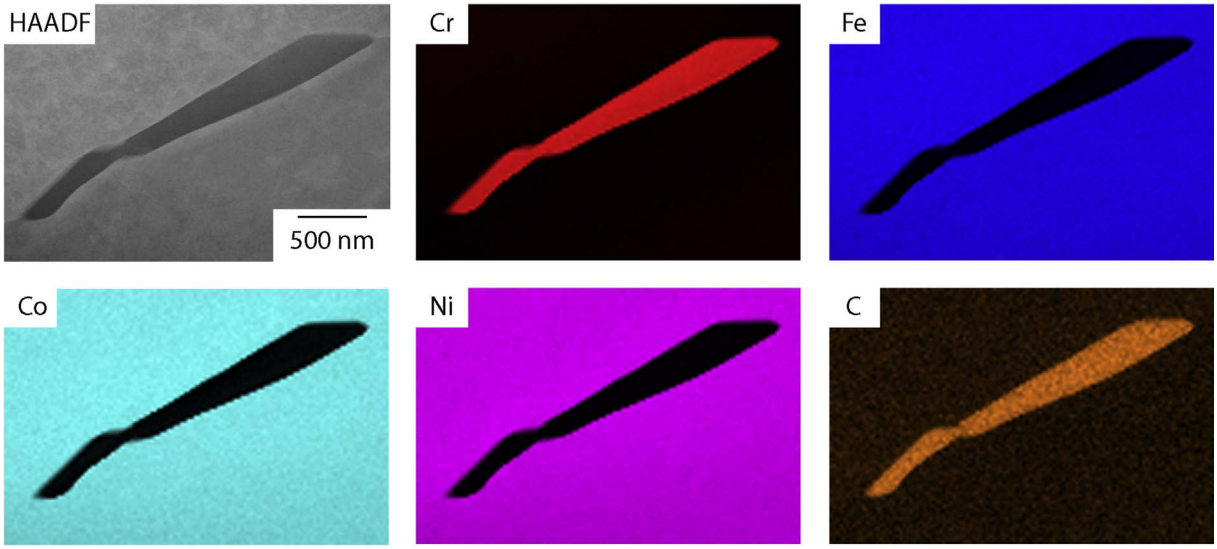

Fig. 6. STEM HAADF image and corresponding EDX distribution maps of a grain boundary precipitate observed in CrFeCoNi following a 1000 h exposure at 700 °C.

example, both CrFeCoNi and $CrMn_{0.5}FeCoNi$ appeared to be single phase *fcc* solid solutions in the as-cast state, based on back scattered electron imaging and laboratory based diffraction patterns. However, elemental distribution maps acquired from the same samples clearly showed inhomogeneities as a result of the solidification process. Such observations are consistent with recent high energy diffraction results that demonstrated that CrFeCoNi solidifies as at least two *fcc* phases with extremely similar lattice parameters [12].

Establishing a single solid solution phase requires the homogenisation of these compositional variations. In CrMnFeCoNi this has been successfully achieved by heat treatments at 1200 °C, which is just below the solidus temperature of the alloy and, therefore, maximises the diffusional distances of the constituent elements per unit time [2,25]. This temperature was chosen primarily as it is close to the operational limit of the quartz glass used to encapsulate the ingots. Despite being at lower homologous temperatures than CrMnFeCoNi, the EDX results presented here showed that the 100 h heat treatments were sufficient to remove the solidification induced microsegregation and achieve a homogeneous single phase state.

Following 1000 h exposures at temperatures of 500, 700 and 900 °C, the microstructures of both CrFeCoNi and $CrMn_{0.5}FeCoNi$ contained no evidence of the sigma phase or any other intermetallic phase. At 900 °C, this result is not surprising as the exposure temperature is above the sigma solvus predicted from thermodynamic modelling [17] and that experimentally observed for the sigma phase in CrMnFeCoNi [1–3]. However, at the lower temperatures, the single *fcc* phase of CrMnFeCoNi is known to decompose [1,2,4] and a similar phase evolution is expected based on thermodynamic predictions [17]. Despite this expectation, the *fcc* phase in the present study was not observed to decompose at either temperature following 1000 h exposures. Small precipitates of a Cr rich phase were observed at the grain boundaries, but these features were conclusively shown to be an $M_{23}C_6$ carbide, which has also been found in CrMnFeCoNi [1,2]. The metallic element compositions of these phases from three different alloys within the $CrMn_xFeCoNi$ series following exposure at 700 °C are given in Table 2. These data were all acquired using STEM based EDX, where the identity of the phase was confirmed using electron diffraction. As can be seen, whilst Cr is the dominant element in both the $M_{23}C_6$ carbide and the sigma phase, there are clear differences in both the Cr concentration and the partitioning of the other elements. The carbide has a Cr content of ~80 at.% or above and contains very low concentrations of Fe, Co and Ni (≤6 at.%), whilst the sigma phase has a Cr content of ~50 at.% and contains appreciable concentrations of both Co and Fe (≥15 at.%). Similar elemental concentrations have been reported for the carbide phases formed in several C modified variants of CrMnFeCoNi following 14 h exposures at 800 °C [26].

Recently, it has been reported that the *fcc* solid solution phase of CrFeCoNi was unstable following exposure at 750 °C for 800 h [16]. This conclusion was reached based on the observation of dark, ~2 μm long, lenticular features in bright field TEM images, which had a difference in lattice parameter of 0.1 Å to the surrounding *fcc* phase. High-resolution imaging failed to find a distinct interface between the matrix and the dark features and so it was suggested that the difference in the lattice parameters indicated atomic clustering and the initial stage of a

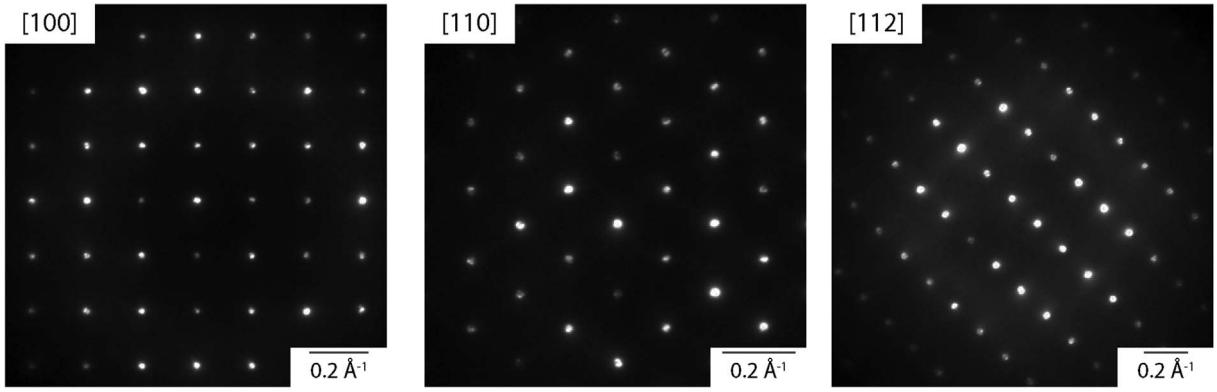

Fig. 7. Selected area diffraction patterns obtained from the grain boundary precipitate observed in CrFeCoNi following a 1000 h exposure at 700 °C.

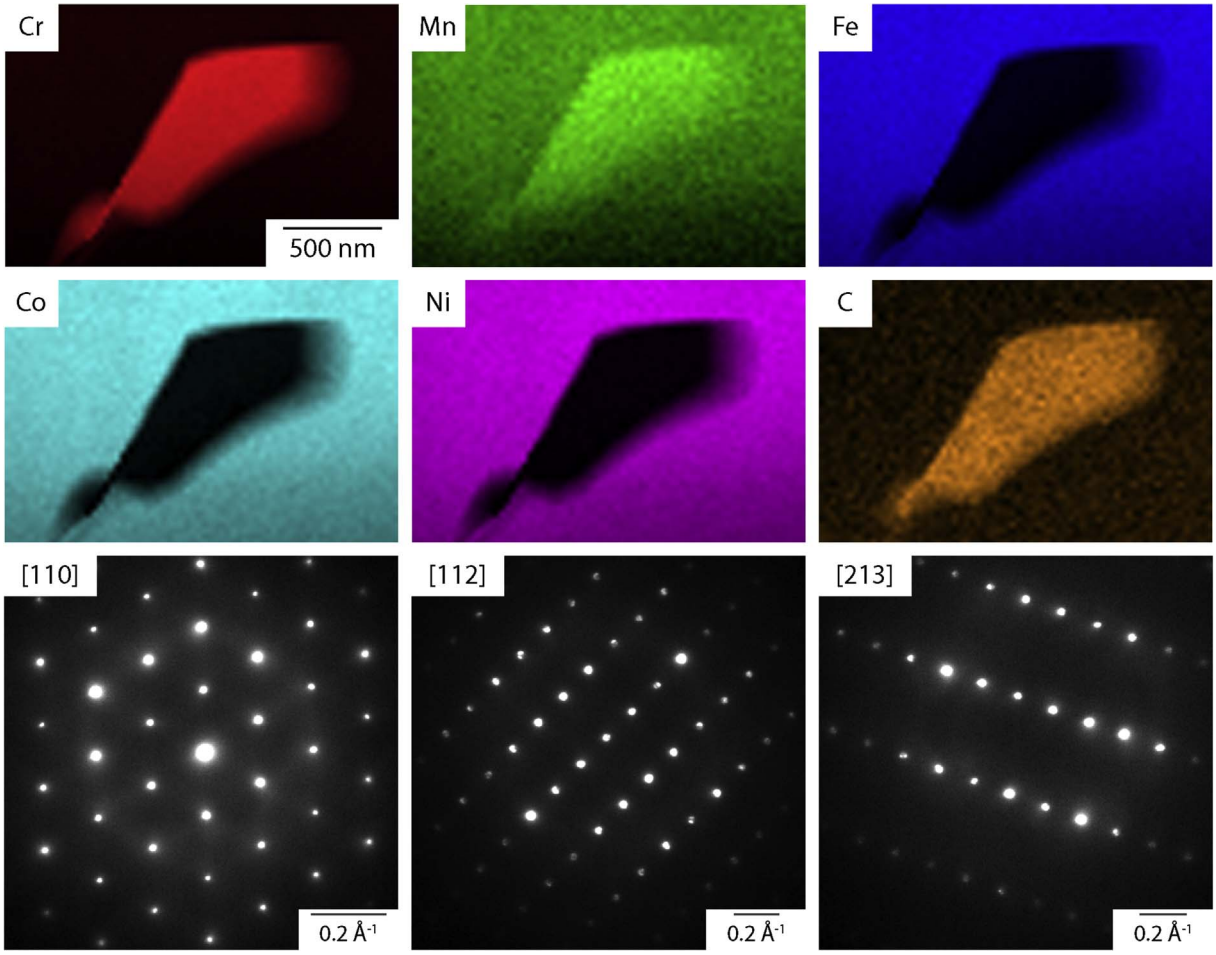

Fig. 8. STEM EDX and electron diffraction patterns corresponding to the carbide phase found in $CrMn_{0.5}FeCoNi$ following heat treatment for 1000 h at 700 °C.

Table 2
Grain boundary phase compositions (metallic elements only) in at.% obtained from STEM EDX data following exposure at 700 °C for 1000 h in the case of CrFeCoNi, $CrMn_{0.5}FeCoNi$ and CrMnFeCoNi from Ref. [1] (standard deviation in each value < 1 at.%) and 12000 h for CrMnFeCoNi from Ref. [2].

Alloy/Phase	Cr	Mn	Fe	Co	Ni
CrFeCoNi	87	–	6	3	3
$M_{23}C_6$					
$CrMn_{0.5}FeCoNi$	80	10	5	3	3
$M_{23}C_6$					
CrMnFeCoNi [1]	79	12	4	2	3
$M_{23}C_6$	46	15	16	16	6
σ					
CrMnFeCoNi [2]	46	12	17	18	7
σ					

phase decomposition, similar to a GP zone in Al-Cu alloys [16]. Similar lenticular features were observed in the present work, both in the homogenised condition and in material that had been exposed for 1000 h. However, these features were found to be compositionally indistinct from the surrounding *fcc* matrix and appeared to be stacking faults. Given that the material in this study was heat treated at a similar temperature to that studied in Ref. [16] but for 25% longer, the present results cast some doubts on the suggestion that this material is producing GP zone like clusters.

The formation of a Cr rich phase along the grain boundaries of a CrFeCoNi based alloy, which also contained a small amount (2.4 at.%) of Al, has been observed following an 800 h exposure at 750 °C [16]. The composition of the grain boundary phase was assessed using SEM based EDX and evaluated as approximately 71Cr-10Fe-10Ni-9Co, from which it was concluded that these features were the sigma phase [16]. However, the results presented here do not support this conclusion, as the reported Cr content is far higher than that of the sigma phase in CrMnFeCoNi and is more consistent with the level found in the $M_{23}C_6$ carbide, Table 2. The concentrations of the other elements, Fe, Ni and Co, are intermediate to the levels discussed above but all of these values should be treated with caution as, given the width of the grain boundary phase (~1 μm), it is conceivable that the SEM probe also interacted with the surrounding material and thus the EDX data contains signal corresponding to the surrounding equiatomic *fcc* matrix. As a consequence, it is believed that the high level of Cr is a key indicator as to the likely identity of the grain boundary phase in Ref. [16], in the absence of conclusive crystallographic information.

As is evident from the discussion above, the results presented in the current study suggest that a reduction in the Mn content from 20 at.% in the CrMnFeCoNi alloy, whilst maintaining all other elements in equiatomic ratios, increases the stability of the solid solution phase against intermetallic phase formation, consistent with previous reports based on shorter duration thermal exposures [10]. A possible reason for this effect can be found by studying the information contained within the constituent ternary phase diagrams. Data from the 700 °C isothermal sections should be considered, as at this temperature, the sigma phase is known to form in CrMnFeCoNi [1–3], whilst the data presented in this study has shown that both $CrMn_{0.5}FeCoNi$ and CrFeCoNi remain stable as single phase solid solutions.

In binary combinations Cr shows very little solubility for either Ni [27] or Co [28] as the temperature decreases from 1200 °C and a significant Cr-rich sigma phase field exists in the Cr-Co system. A sigma

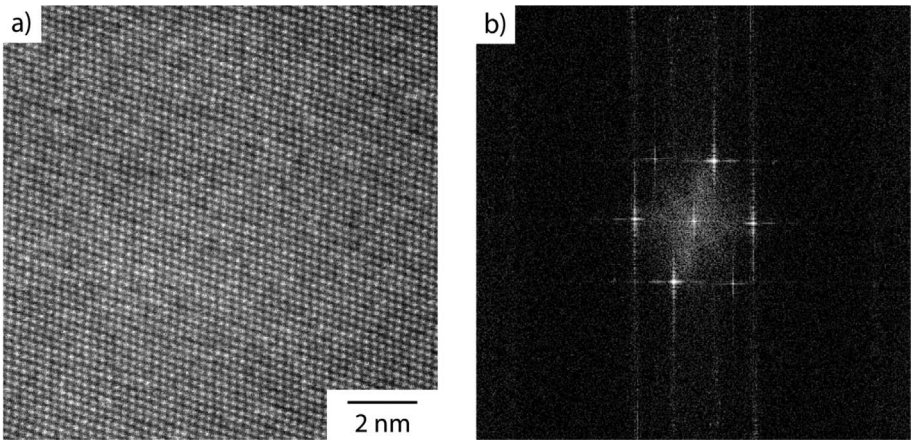

Fig. 9. a) HAADF image of the grain interior of CrFeCoNi following a 1000 h exposure at 700 °C, b) corresponding Fourier transform.

phase field also exists in the Cr-Fe system, forming as the miscibility gap between Cr and Fe begins to open at a temperature of ~840 °C [29]. In ternary space, a sigma phase field is present in the Co-Cr-Fe system at 700 °C and extends across the entire isothermal section. This phase field has a fairly narrow compositional range at the Fe rich end, ~5 at.%, but widens significantly with the addition of Co, ~10 at.% and an equiatomic CrFeCo alloy would lie in a two phase field with equilibrium between sigma and an *fcc* phase [30]. Consequently, it might be expected that the sigma phase would form in the CrFeCoNi quaternary alloy but, based on the experimental results presented here and the other relevant ternary phase diagrams [31], the large solubility range of the *fcc* phase in the Fe-Co-Ni system at 700 °C must enable the Cr to be retained in solution when present in equiatomic concentrations.

The addition of Mn has a pronounced effect on the size of the sigma phase field, causing a significant enlargement, as can be seen in the Cr-Fe-Mn system, [32]. In the absence of Mn, the width of the sigma phase is ~5 at.%, whilst the addition of Mn allows this to broaden to a maximum of around ~20 at.% when the Mn concentrations are above 10 at.%. This effect is far more pronounced than that caused by relatively low concentrations of Co. Extending these concepts to the equiatomic CrMnFeCoNi alloy, it can be envisaged that the presence of Co and Mn, each in concentrations of 20 at.%, would result in a reasonably large sigma phase field. Similarly, if the Mn content were reduced then, following the same logic, the level of Fe solubility in the sigma phase would be expected to decrease, reducing the size of the phase field.

In an attempt to explore this hypothesis in more detail, unconstrained thermodynamic calculations were performed using Thermocalc and the TCHEA1 database, which produced phase diagrams consistent with those presented in Ref. [17]. The predicted compositions of the *fcc* solid solution phase and the sigma phase in the CrFeCoNi, $CrMn_{0.5}FeCoNi$ and CrMnFeCoNi alloys were considered as a function of temperature to see if variations in Mn content influenced the elemental partitioning. In all of the alloys, the sigma phase was predicted to form at temperatures between 650 and 590 °C with a corresponding decrease in the Cr content of the *fcc* solid solution phase. Whilst these predictions did not correlate well with experimental observations, where the sigma phase has only been observed in CrMnFeCoNi, they did suggest a change in phase composition with the Mn content, Table 3. In the absence of Mn the sigma phase was predicted to be Cr-Fe-Co based, whereas in the equiatomic quinary alloy, the sigma phase was predicted to be Cr-Fe-Mn based with relatively little Co content. The alteration in the constitution of the sigma phase was predicted to occur when the Mn content of the alloy was between that of $CrMn_{0.5}FeCoNi$ and CrMnFeCoNi. It is possible that this predicted change in composition of the sigma phase could also alter its propensity to form and, hence, rationalise the observed influence of Mn on its occurrence in the $CrMn_xFeCoNi$ series. However, current

Table 3
Thermodynamic predictions using the TCHEA1 database of the sigma phase composition in the $CrMn_xFeCoNi$ system at 550 °C (at.%).

Alloy	Cr	Mn	Fe	Co	Ni
CrMnFeCoNi	38	26	30	5	1
$CrMn_{0.5}FeCoNi$	56	2	18	20	4
CrFeCoNi	57	–	14	23	6

thermodynamic predictions of this system should be treated with extreme caution, as a number of key inconsistencies with experimental data exist. First, as mentioned above, the calculations predicted the formation of the sigma phase in CrFeCoNi, $CrMn_{0.5}FeCoNi$ and CrMnFeCoNi, whilst, to date it has only been observed in CrMnFeCoNi. Second, the sigma solvus in CrMnFeCoNi was predicted to be ~600 °C, whereas experimental studies have shown this to be closer to 800 °C [1,2]. Third, the predicted composition of the sigma phase in CrMnFeCoNi is markedly different to that measured experimentally. As can be seen from Table 2, the measured composition of the sigma phase was found to have relatively high Co and Fe contents and slightly lower concentrations of Mn. This is in contrast to the calculated composition, which predicted a much greater concentration of Mn and relatively little Co in the sigma phase. Whilst assessing the fidelity of the thermodynamic predictions of this system, it ought to be pointed out that a Cr *bcc* solid solution, a NiMn intermetallic and a FeCo B2 phase are predicted at temperatures below 500 °C, which match the phases observed in CrMnFeCoNi following 12000 h at 500 °C [2]. As such, it would appear that a key issue for the current database is the lack of data relating to the stability of the sigma phase in Mn containing systems, most notably the Co-Cr-Mn and the Co-Fe-Mn ternaries, which is in agreement with the conclusion reached by Bracq et al. [17].

5. Conclusions

This study has considered the influence of Mn on the stability of the single *fcc* solid solution phase in $CrMn_xFeCoNi$ HEAs. The microstructures of CrFeCoNi and $CrMn_{0.5}FeCoNi$ have been characterised following homogenisation at 1200 °C for 100 h and 1000 h heat treatments at 500, 700 and 900 °C and compared to existing literature data for CrMnFeCoNi.

In the homogenised state, both alloys exhibited a single *fcc* structured solid solution phase, with an even distribution of the constituent elements. Following long-term heat treatment at each of the three temperatures, Cr rich phases were observed to have formed on the grain boundaries of all alloys. Detailed analysis of these precipitates using STEM EDX and electron diffraction patterns showed that they were also enriched in C and had an *fcc* unit cell with a lattice parameter of ~10.6 Å. The quantified EDX data of these phases were consistent with

similar features previously found in CrMnFeCoNi and, consequently, it was concluded that these particles were an $M_{23}C_6$ carbide.

However, unlike CrMnFeCoNi, no intermetallic phases were observed to have formed in either CrFeCoNi or $CrMn_{0.5}FeCoNi$ during the 1000 h heat treatments. It is the authors' opinion that the formation of a carbide does not portray an instability of the solid solution phase, and, therefore, in contrast to some recent reports, the solid solution phases of these alloys are believed to be stable within the time and temperature limits of the current dataset.

Thus, the experimental data presented here clearly shows that Mn has a destabilising influence on the single *fcc* phase of $CrMn_xFeCoNi$ HEAs. Specifically, the sigma phase will form when Mn is present above a certain concentration, which is between 11.1 and 20 at.% Mn in $CrMn_xFeCoNi$ alloys.

Acknowledgements

The authors wish to acknowledge the support from HM Government (UK) for the provision of the funds for the FEI Titan G2 80-200 S/TEM associated with research capability of the Nuclear Advanced Manufacturing Research Centre. HJS and NGJ would like to acknowledge the support of the EPSRC/Rolls-Royce Strategic Partnership under EP/M005607/1. The underlying experimental data that supports this research is available from: https://doi.org/10.17863/CAM.13372.

References

[1] E.J. Pickering, R. Muñoz-Moreno, H.J. Stone, N.G. Jones, Precipitation in the equiatomic high-entropy alloy CrMnFeCoNi, Scr. Mater. 113 (C) (2016) 106–109.
[2] F. Otto, A. Dlouhy, K.G. Pradeep, M. Kuběnová, D. Raabe, G. Eggeler, E.P. George, Decomposition of the single-phase high-entropy alloy CrMnFeCoNi after prolonged anneals at intermediate temperatures, Acta Mater. 112 (C) (2016) 40–52.
[3] N.D. Stepanov, D.G. Shaysultanov, M.S. Ozerov, S.V. Zherebtsov, G.A. Salishchev, Second phase formation in the CoCrFeNiMn high entropy alloy after recrystallization annealing, Mater. Lett. 185 (C) (2016) 1–4.
[4] B. Schuh, F. Mendez-Martin, B. Völker, E.P. George, H. Clemens, R. Pippan, A. Hohenwarter, Mechanical properties, microstructure and thermal stability of a nanocrystalline CoCrFeMnNi high-entropy alloy after severe plastic deformation, Acta Mater. 96 (C) (2015) 258–268.
[5] Y.-F. Kao, T.-J. Chen, S.-K. Chen, J.-W. Yeh, Microstructure and mechanical property of as-cast, -homogenized, and -deformed AlxCoCrFeNi ($0 \le x \le 2$) high-entropy alloys, J. Alloy Compd. 488 (1) (2009) 57–64.
[6] W.-R. Wang, W.-L. Wang, S.-C. Wang, Y.-C. Tsai, C.-H. Lai, J.-W. Yeh, Effects of Al addition on the microstructure and mechanical property of AlxCoCrFeNi high-entropy alloys, Intermetallics 26 (C) (2012) 44–51.
[7] T.-T. Shun, L.-Y. Chang, M.-H. Shiu, Microstructure and mechanical properties of multiprincipal component CoCrFeNiMox alloys, Mater. Charact. 70 (C) (2012) 63–67.
[8] S. Guo, C. Ng, Z. Wang, C.T. Liu, Solid solutioning in equiatomic alloys: limit set by topological instability, J. Alloy Compd. 583 (C) (2014) 410–413.
[9] A.K. Singh, A. Subramaniam, On the formation of disordered solid solutions in multi-component alloys, J. Alloy Compd. 587 (C) (2014) 113–119.
[10] M.S. Lucas, G.B. Wilks, L. Mauger, J.A. Muñoz, O.N. Senkov, E. Michel, J. Horwath, S.L. Semiatin, M.B. Stone, D.L. Abernathy, E. Karapetrova, Absence of long-range chemical ordering in equimolar FeCoCrNi, Appl. Phys. Lett. 100 (25) (2012) 251907.
[11] J. Cornide, M. Calvo-Dahlborg, S. Chambreland, L. Asensio Dominguez, Z. Leong, U. Dahlborg, A. Cunliffe, R. Goodall, I. Todd, Combined atom probe tomography and TEM investigations of CoCrFeNi, CoCrFeNi-Pd x(x = 0.5, 1.0, 1.5) and CoCrFeNi-Sn, Acta Phys. Pol. A 128 (4) (2015) 557–561.
[12] U. Dahlborg, J. Cornide, M. Calvo-Dahlborg, T.C. Hansen, A. Fitch, Z. Leong, S. Chambreland, R. Goodall, Structure of some CoCrFeNi and CoCrFeNiPd multi-component HEA alloys by diffraction techniques, J. Alloy Compd. 681 (C) (2016) 330–341.
[13] E.J. Pickering, N.G. Jones, High entropy alloys: a critical assessment of their founding principles and future prospects, Int. Mater. Rev. 61 (2016) 183–202.
[14] D.B. Miracle, O.N. Senkov, A critical review of high entropy alloys and related concepts, Acta Mater. 122 (C) (2017) 448–511.
[15] R. Kozak, A. Sologubenko, W. Steurer, Single-phase high-entropy alloys–an overview, Z Krist. 230 (1) (2015) 55–68.
[16] F. He, Z. Wang, Q. Wu, J. Li, J. Wang, C.T. Liu, Phase separation of metastable CoCrFeNi high entropy alloy at intermediate temperatures, Scr. Mater. 126 (2017) 15–19.
[17] G. Bracq, M. Laurent-Brocq, L. Perrière, R. Pirès, J.-M. Joubert, I. Guillot, The fcc solid solution stability in the Co-Cr-Fe-Mn-Ni multi-component system, Acta Mater. 128 (2017) 327–336.
[18] F. Otto, Y. Yang, H. Bei, E.P. George, Relative effects of enthalpy and entropy on the phase stability of equiatomic high-entropy alloys, Acta Mater. 61 (7) (2013) 2628–2638.
[19] A. Gali, E.P. George, Tensile properties of high- and medium-entropy alloys, Intermetallics 39 (C) (2013) 74–78.
[20] G. Laplanche, O. Horst, F. Otto, G. Eggeler, E.P. George, Microstructural evolution of a CoCrFeMnNi high-entropy alloy after swaging and annealing, J. Alloy Compd. 647 (C) (2015) 548–557.
[21] N.D. Stepanov, D.G. Shaysultanov, G.A. Salishchev, M.A. Tikhonovsky, E.E. Oleynik, A.S. Tortika, O.N. Senkov, Effect of V content on microstructure and mechanical properties of the CoCrFeMnNiVx high entropy alloys, J. Alloy Compd. 628 (C) (2015) 170–185.
[22] G. Laplanche, A. Kostka, C. Reinhart, J. Hunfeld, G. Eggeler, E.P. George, Reasons for the superior mechanical properties of medium-entropy CrCoNi compared to high-entropy CrMnFeCoNi, Acta Mater. 128 (2017) 292–303.
[23] J.X. Fu, C.M. Cao, W. Tong, Y.X. Hao, L.M. Peng, The tensile properties and serrated flow behavior of a thermomechanically treated CoCrFeNiMn high-entropy alloy, Mater. Sci. Eng. A 690 (2017) 418–426.
[24] F. Otto, A. Dlouhy, C. Somsen, H. Bei, G. Eggeler, E.P. George, The influences of temperature and microstructure on the tensile properties of a CoCrFeMnNi high-entropy alloy, Acta Mater. 61 (15) (2013) 5743–5755.
[25] L.R. Owen, H.Y. Playford, H.J. Stone, M.G. Tucker, N.G. Jones, A new approach to the analysis of short-range order in alloys using pair distribution functions, Acta Mater. 122 (2017) 11–18.
[26] N.D. Stepanov, N.Y. Yurchenko, M.A. Tikhonovsky, G.A. Salishchev, Effect of carbon content and annealing on structure and hardness of the CoCrFeNiMn-based high entropy alloys, J. Alloy Compd. 687 (C) (2016) 59–71.
[27] P. Turchi, L. Kaufman, Z. Liu, Modelling of Ni-Cr-Mo based alloys: part I - phase stability, Calphad 30 (1) (2006) 70–87.
[28] H. Okamoto, Co-Cr, J. Phase Equilb. 24 (4) (2003) 377–378.
[29] S. Chen, J. Zhang, L. XG, K. Chou, Y. Chang, Application of Graham scan algorithm in binary phase diagram calculation, J. Phase Equilib. Diffus. 27 (2) (2006) 121–125.
[30] G. Raynor, V. Rivlin, Co-Cr-Fe, Phase Equilibria in Iron Ternary Alloys, (1988), pp. 213–230.
[31] G. Raynor, V. Rivlin, Co-Fe-Ni, Phase Equilibria in Iron Ternary Alloys, (1988), pp. 247–255.
[32] G. Raynor, V. Rivlin, Cr-Fe-Mn Isothermal Section at 750°C, Phase Equilibria in Iron Ternary Alloys, (1988), pp. 288–299.